

Aluminum Tris(2,6-diphenylphenoxide)-ArCOCl Complex for Nucleophilic Dearomatic Functionalization

Susumu Saito, Toshihiko Sone, Masaaki Murase, and Hisashi Yamamoto*

Graduate School of Engineering, Nagoya University
CREST, Japan Science and Technology Corporation (JST)
Chikusa, Nagoya 464-8603, Japan

Received April 25, 2000

Recently, we demonstrated the nucleophilic dearomatization of benzaldehyde (PhCHO) complexed with aluminum tris(2,6-diphenylphenoxide) (ATPH) (Figure 1),¹ which proceeded smoothly with a variety of nucleophiles.² Unfortunately, however, conjugate addition to the ATPH-PhCHO complex did not proceed effectively with smaller nucleophiles (Scheme 1). For example, MeLi and the lithium enolates of methyl acetate undergo 1,2-addition predominantly. The lithium enolates of several ketones, methyl propionate, *tert*-butyl acetate, PhLi, and vinyl- and allyllithiums give equal amounts of 1,2- and 1,6-adducts. In sharp contrast, treatment of a toluene solution of ATPH (1.1 equiv) with benzoyl chloride (PhCOCl; 1.0 equiv) at $-78\text{ }^{\circ}\text{C}$, followed by addition of MeLi (3.0 equiv)³ and workup with concentrated HCl gives 1,6- and 1,4-adducts **1a** and **1b** in a ratio of 2.6:1 in 99% isolated yield (Scheme 1).

Nucleophiles that add in a 1,6-manner to ATPH-PhCOCl include Grignard reagents (*i*-PrMgBr and *t*-BuMgCl), which are ineffective for the conjugate addition to the ATPH-PhCHO complex. Figure 2 shows that enhanced regioselectivities (1,6- vs 1,2-addition) are achieved with the ATPH-PhCOCl complex. Addition products can be isolated as acids or esters by altering workup conditions. In each of these cases, 1,2-adduct could not be detected by ¹H NMR analysis.

Insight regarding the change in product distribution in the two types of complexes may be derived from a comparison of their X-ray crystal structures. The X-ray crystal structure of ATPH-PhCHO, Figure 3a,⁴ shows one face of the extended π -system to be relatively exposed, at least in the region distal to the carbonyl group. On the other hand, the X-ray crystal structure of ATPH-PhCOCl,⁴ Figure 3b, revealed that two of the phenyl rings (black) of ATPH and the flat PhCOCl form a sandwich structure, rendering the C=O highly congested. The C=O of ATPH-PhCOCl has a single bond-like character. The Al–O=C bond of 1.235(4) Å is longer than that of Al–O=CHPh (1.14(1) Å).⁵ This is consistent with the FT-IR measurement of the ATPH-PhCOCl and ATPH-PhCHO complexes in solution (CD₂Cl₂, $-40\text{ }^{\circ}\text{C}$). The frequency of the carbonyl of ATPH-PhCOCl is shifted to a lower frequency as a result of enhanced conjugation relative to that of the free substrates by 42 cm⁻¹.⁶ The ATPH-PhCHO complex,

(1) (a) Saito, S.; Yamamoto, H. *Chem. Commun.* **1997**, 1585. (b) Yamamoto, H.; Saito, S. *Pure Appl. Chem.* **1999**, *71*, 235. (c) Saito, S.; Yamamoto, H. *Chem. Eur. J.* **1999**, *5*, 1959.

(2) For preliminary results concerning nucleophilic addition to aromatic rings using ATPH, see: (a) Maruoka, K.; Ito, M.; Yamamoto, H. *J. Am. Chem. Soc.* **1995**, *117*, 9091. (b) Saito, S.; Shimada, K.; Yamamoto, H. Marigorta, E. M.; Fleming, I. *Chem. Commun.* **1997**, 1299. (c) Saito, S.; Sone, T.; Yamamoto, H. *Synlett* **1999**, 81.

(3) The use of less nucleophile (1.1–2.5 equiv) gives the corresponding product in lower yield.

(4) The single-crystal structures of ATPH-PhCHO and ATPH-PhCOCl were established for the first time in this paper. See Supporting Information for details.

(5) The average bond length of C=O in free RCOCl is ca. 1.18 Å. The C=O of RCHO has a similar average length of ca. 1.22 Å. See also ref 1 in the Supporting Information.

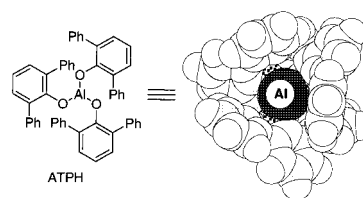


Figure 1. Molecular structure of ATPH.

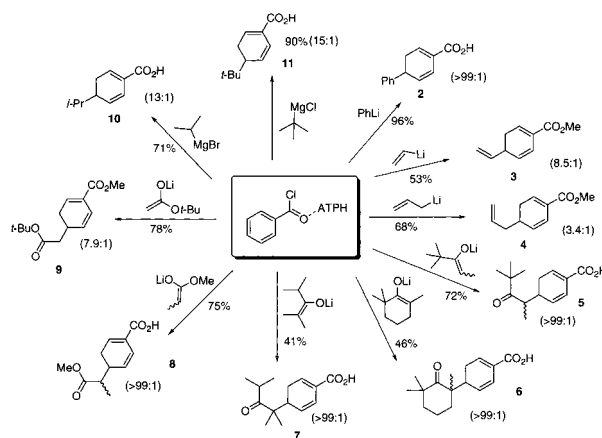


Figure 2. Conjugate addition of various nucleophiles using the ATPH-PhCOCl. The values in parentheses are ratios of 1,6- and 1,4-adducts, which were determined by ¹H NMR analysis. Combined yields of 1,6- and 1,4-adducts are indicated. Acids and esters are obtained with the following conditions: $-78\text{ }^{\circ}\text{C}$ to room temperature; acid, concentrated HCl; ester, Et₂O solution of HCl, followed by MeOH.

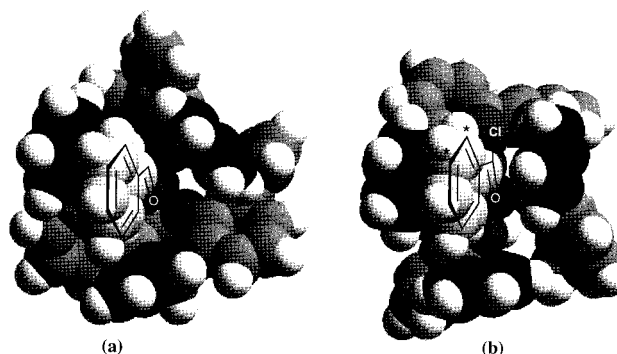
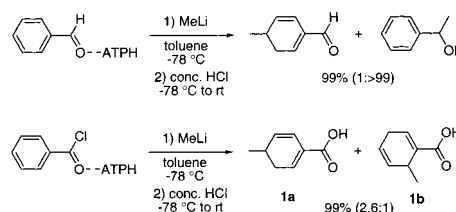


Figure 3. The X-ray crystal structures of (a) ATPH-PhCHO and (b) ATPH-PhCOCl.

Scheme 1



on the other hand, exhibits no detectable shift. In fact, the π -deficiency of PhCOCl is significantly enhanced by complex-

(6) For benzoyl chlorides, an unequal intensity of doublet is usually seen in the C=O region. A second band is due to the Fermi resonance involving the stretch of the overtone of the Ph–C which interacts with the carbonyl stretch. IR frequency: PhCHO (1708 cm⁻¹); ATPH-PhCHO (1708 cm⁻¹); PhCOCl (1770 (C=O stretch) and 1728 (due to the Fermi resonance) cm⁻¹); ATPH-PhCOCl (1728 cm⁻¹). See also ref 2 in the Supporting Information.

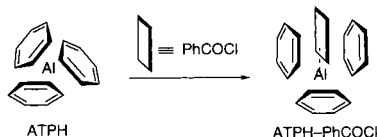


Figure 4. Schematic depiction of the induced conformational changes of ATPH as a “molecular tweezer” for effective inclusion of PhCOCl. The three benzene rings correspond to the darkened phenyls in Figure 3b.

ation with ATPH. ^{13}C NMR measurements (75 MHz, CD_2Cl_2 , -30°C) show downfield shifts ($\Delta\delta$) for the carbonyl carbon from free to bound substrates of 9.49 ppm for ATPH-PhCHO and 18.0 ppm for ATPH-PhCOCl.⁷ The π -stacking between two π -donors (ATPH phenyls) and one π -acceptor (complexed PhCOCl) involving the carbonyl carbon may act as a “molecular tweezer”⁸ to stabilize the ATPH-PhCOCl complex (Figure 4). The interaction does not seem to be the primary binding force, but rather is induced upon intrinsic Lewis acid–base complexation.⁹ This aspect was further demonstrated by a ^{13}C NMR (CD_2Cl_2 , -78°C to room temperature) competition experiment using a 1:1:1 mixture of ATPH, PhCHO, and PhCOCl. The analysis shows $K_{\text{PhCOCl}}/K_{\text{PhCHO}} = ([\text{ATPH}\cdot\text{PhCOCl}]/[\text{ATPH}\cdot\text{PhCHO}])([\text{PhCHO}]_{\text{free}}/[\text{PhCOCl}]_{\text{free}}) < 3.5 \times 10^{-3}$,¹⁰ suggesting that PhCOCl forms complexes that are less stabilized than those of PhCHO by more than 14 kJ mol⁻¹ (at 298 K). It should be emphasized that the relative destabilization, i.e., the higher reactivity of ATPH-PhCOCl, compared with ATPH-PhCHO, might be compensated for to some extent by the formation of the “molecular tweezer”.

When *t*-BuLi was used for the *tert*-butylation of ATPH-PhCHO, the 1,6-adduct, but no 1,4-adduct, was produced.^{2a} This could be ascribed to the distinctive structure of ATPH-PhCHO, which is not driven to π -sandwiching (Figure 3a). The two ortho positions of ATPH-PhCHO are sterically encumbered to an equal degree, while one of the two ortho positions (the asterisked ortho position: 1,4-addition site) of ATPH-PhCOCl is sterically deshielded due to the sandwich structure (Figure 3b). Alkylolithiums are prone to 1,4-addition with ATPH-PhCOCl in the order MeLi > BuLi > *s*-BuLi > *t*-BuLi,¹¹ although they show a general preference for 1,6-selectivity. Unexpectedly, we observed complete regiochemical reversal according to the size of RLi upon addition to acid chloride complexes **12** and **14**: 1,6-selectivity predominated with *t*-BuLi to give **13c** and **15d**, whereas MeLi underwent 1,4-addition exclusively to give **13a,b** and **15a,b** (Scheme 2).

(7) ^{13}C NMR (75 MHz, CD_2Cl_2 , -30°C) chemical shifts: PhCHO (191.9 ppm); ATPH-PhCHO (201.4 ppm); PhCOCl (168.0 ppm); and ATPH-PhCOCl (185.0 ppm). We can exclude the species $[\text{PhC}\equiv\text{O}^+][\text{ATPH}\cdot\text{Cl}^-]$ to account for this significant downfield shift, since a single crystal of ATPH-PhCOCl was grown in CH_2Cl_2 -hexane at -20°C to give the structure shown in Figure 3b.

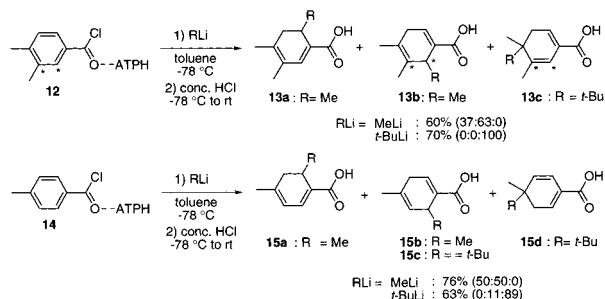
(8) The two phenyl rings of ATPH which form the π -sandwich are separated by ca. 7.0 Å. This value is identical to the distance in “molecular tweezers” which can include aromatic guests by interactions between two π -donors and one π -acceptor, see: Zimmerman, S. C.; VanZyl, C. M.; Hamilton, G. S. *J. Am. Chem. Soc.* **1989**, *111*, 1373. See also ref 3 in the Supporting Information.

(9) Zimmerman (ref 8) pointed out that cooperative π -stacking with an electron donor–acceptor component can contribute to complex stability if hydrophobic forces or hydrogen bonding is present. In our case, the Lewis acid–base coordination may substitute for these forces and bonding.

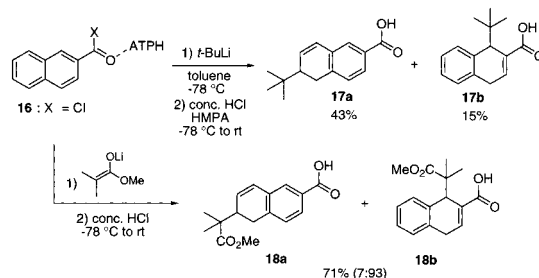
(10) Although we encountered an experimental limit for measuring $K_{\text{PhCOCl}}/K_{\text{PhCHO}}$, the preferred order of binding to ATPH is $\text{PhCO}_2\text{Me} > \text{PhCOCl}$, and the relative binding constant of PhCO_2Me and PhCHO is $K_{\text{PhCO}_2\text{Me}}/K_{\text{PhCHO}} = 3.5 \times 10^{-3}$. In these competition experiments using ATPH, we always observed a set of two chemical shifts, each corresponding to free and bound substrates, due to slow exchange at the NMR time scale.

(11) Exposure of ATPH-PhCOCl to these nucleophiles gives 1,6- and 1,4-product ratios of 2.6:1 (MeLi), 4.5:1 (*n*-BuLi), 14:1 (*s*-BuLi), and 39:1 (*t*-BuLi). A similar regiochemical trend was obtained previously using the ATPH- α -naphthaldehyde complex (see ref 2a).

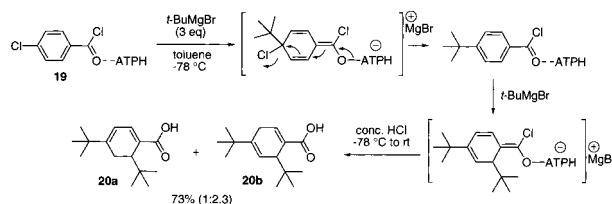
Scheme 2



Scheme 3



Scheme 4



As shown in Figure 3b, complex **12** should orient itself so that the *m*-methyl substituted carbon occupies the less-congested meta site which is marked with an asterisk. Attack at both ortho positions of **12** is unfavorable, and hence bulky *t*-BuLi suffers 1,6-addition to give **13c** exclusively (Scheme 2). This observation is in contrast to the formation of 1,6-adduct **15d** accompanied by a small amount of 1,4-adduct **15c**. The ratio of two different 1,4-adducts **13a,b** could be explained along similar lines (Scheme 2): the asterisked ortho position, which is less congested than the other ortho position, is selectively methylated.

The ATPH- β -naphthaldehyde complex ($X = \text{H}$, Scheme 3) did not undergo conjugate addition even with *t*-BuLi. However, the reaction proceeded smoothly with the use of acid chloride complex **16**. Of particular interest is the novel 1,8-selectivity to give **17a** (Scheme 3). In marked contrast, 1,4-addition predominated with the lithium enolate of 2-methylpropionate to give **18b** in 66% yield (Scheme 3).

Another striking advantage of the present method can be seen in the reaction of 4-chlorobenzoic acid chloride **19** with *t*-BuMgBr (3equiv) (Scheme 4). This facilitates a tandem 1,6-addition–chloride elimination–rearromatization–1,4-addition sequence, i.e., in situ double conjugate addition, to give **20a** and **20b** in 73% yield.

Supporting Information Available: Experimental procedures and analytical and spectral data for all new compounds (PDF). This material is available free of charge via the Internet at <http://pubs.acs.org>.

JA0014382